# Binding model for eriodictyol to Jun-N terminal kinase and its anti-inflammatory signaling pathway

*Eunjung Lee[1], Ki-Woong Jeong[1], Areum Shin[1], Bonghwan Jin[1], Hum Nath Jnawali[1], Bong-Hyun Jun[1], Jee-Young Lee[2], Yong-Seok Heo[3] & Yangmee Kim[1,*]*

[1]Department of Bioscience and Biotechnology, Bio-Molecular Informatics Center, Institute of KU Biotechnology, Konkuk University, Seoul 143-701, [2]Drug Discovery Team, Bioinformatics & Molecular Design Research Center, Seoul 120-749, [3]Department of Chemistry, Konkuk University, Seoul 143-701, Korea

**The anti-inflammatory activity of eriodictyol and its mode of action were investigated. Eriodictyol suppressed tumor necrosis factor (mTNF)-α, inducible nitric oxide synthase (miNOS), interleukin (mIL)-6, macrophage inflammatory protein (mMIP)-1, and mMIP-2 cytokine release in LPS-stimulated macrophages. We found that the anti-inflammatory cascade of eriodictyol is mediated through the Toll-like Receptor (TLR)4/CD14, p38 mitogen-activated protein kinases (MAPK), extracellular-signal-regulated kinase (ERK), Jun-N terminal kinase (JNK), and cyclooxygenase (COX)-2 pathway. Fluorescence quenching and saturation-transfer difference (STD) NMR experiments showed that eriodictyol exhibits good binding affinity to JNK, $8.79 \times 10^5$ M$^{-1}$. Based on a docking study, we propose a model of eriodictyol and JNK binding, in which eriodictyol forms 3 hydrogen bonds with the side chains of Lys55, Met111, and Asp169 in JNK, and in which the hydroxyl groups of the B ring play key roles in binding interactions with JNK. Therefore, eriodictyol may be a potent anti-inflammatory inhibitor of JNK. [BMB Reports 2013; 46(12): 594-599]**

## INTRODUCTION

Inflammation is an early response of vascular tissues to infection, injuries, and harmful stimuli such as pathogens and irritants, and it is associated with nonspecific immune responses for neutralizing invaders and repairing damaged cells, and finally it initiates healing processes (1). Inflammation is caused by the binding of a pathogen to toll-like receptor (TLR) 4 and CD14 receptors, which activates cellular signaling (2). Since nitric oxide (NO) is one of the inflammatory mediators, in-

flammation is characterized by the secretion of NO, and modulation of NO is considered a possible treatment for inflammatory disease (3). The increase in inducible nitric oxide synthase (iNOS) and cyclooxygenase (COX)-2 causes cell damage following the increased production of NO and prostaglandins (PGs) (4). Suppressing the induction of COX-2 is a new strategy in the prevention of inflammation and COX-2 expression is also related to the activities of many intracellular signaling proteins, such as extracellular signal-regulated kinase (ERK), mitogen-activated protein kinase (MAPK), and Jun-N terminal kinase (JNK) (5).

Many research studies support the beneficial association between health and the intake of fruits and vegetables, and polyphenols in fruits and vegetables are known to induce functional benefits (6). Among polyphenols, flavonoids are naturally occurring compounds that are ubiquitous in plants and vegetables. Flavonoids have been recognized to exhibit biological effects in various diseases, including effects that are anti-hepatotoxic, anti-atherogenic, anti-allergic, and anti-cancerous, in addition to their anti-inflammatory activity (7). Flavonoids are known to interact with the ATP-binding sites of tyrosine kinase and serine kinase, resulting in the inhibition of these proteins (8). Many lines of evidence suggest a direct role for flavonoids in modulating the inflammatory response *in vitro* or in cellular models. Quercetin, apigenin, luteolin, naringenin, and kaempferol suppress NO production in lipopolysaccharide (LPS)- or cytokine-stimulated macrophages, whereas catechin and a few flavanones were not active in reducing NO production in LPS-stimulated macrophages (9). In our previous study, we reported anti-inflammatory activities of amentoflavone found in *Ginko biloba* and *Hypericum perforatum* and systematically determined the signal transduction pathways (10).

Eriodictyol is an interesting flavonoid because it is distributed in common foods and shows beneficial biological activities. Several fruits and vegetables express eriodictyol, especially lemons (11, 12). We have shown that eriodictyol is a potent antimicrobial inhibitor of *Staphylococcus aureus* β-ketoacyl acyl carrier protein synthase III (KAS III), with strong binding affinities of $2.01 \times 10^5$ M$^{-1}$ as well as high antimicrobial activities against *S. aureus* and 4 Methicillin-resistant

*Staphylococcus aureus* (MRSA) strains (13). In addition, eriodictyol was selected as one of the *Enterococcus faecalis* KAS III inhibitors using docking studies, and it displays antimicrobial activity against *E. faecalis* and vancomycin-resistant *E. faecalis* (VREF) (14). Eriodictyol was found to suppress NO production, nuclear factor (NF)-κB activation, and MAPK phosphorylation in mouse macrophages (15). In this study, we further investigated the anti-inflammatory activities of eriodictyol and its mechanism in mouse macrophages. Herein, we report that eriodictyol exhibits anti-inflammatory activity to inhibit production of LPS-stimulated pro-inflammatory cytokines and systematically present our understanding of the mechanisms by which it activated TLR4/CD14 following p38 MAPK, ERK1/2, JNK, and COX-2 regulation. We determined interactions between JNK and eriodictyol using fluorescence quenching analysis and saturation-transfer difference (STD)-NMR spectroscopy. We also propose a model of JNK binding with eriodictyol using the results of our docking study.

## RESULTS

### Cytotoxicity in RAW264.7, NIH3T3, and HaCaT cells

In order to determine the nontoxic concentration of eriodictyol in RAW264.7, NIH3T3, and HaCaT cells, we investigated cytotoxicity by MTT assay, as shown in Fig. 1. An eriodictyol concentration of up to 25 μM did not affect cell viability; even at an eriodictyol concentration of up to 100 μM, the survival rate was greater than 70% in mouse macrophage cells. The survival rates of NIH3T3 cells were 87.4%, 76.6%, and 48.4% at 25, 50, and 100 μM eriodictyol, respectively. Interestingly, 100 μM of eriodictyol did not affect cell survival at all for HaCaT cells.

## Quantification of nitrite production in LPS-stimulated RAW264.7 cells

We investigated inhibition of NO production at 1 μM, 2.5 μM, 5 μM, 10 μM, and 20 μM eriodictyol. The 2.5 μM eriodictyol resulted in more than twice the inhibition compared to cells that were not treated with eriodictyol. Eriodictyol completely inhibited NO production at 20 μM (Fig. 2A), a concentration of eriodictyol that was nontoxic to RAW264.7, NIH3T3, and HaCaT cells (Fig. 1).
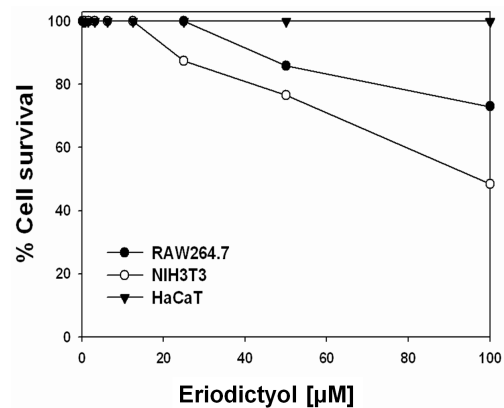


**Fig. 1.** Dose-response curves of eriodictyol for cytotoxicity toward macrophage-derived RAW264.7 (●), NIH3T3 (○), and HaCaT (▼) cells
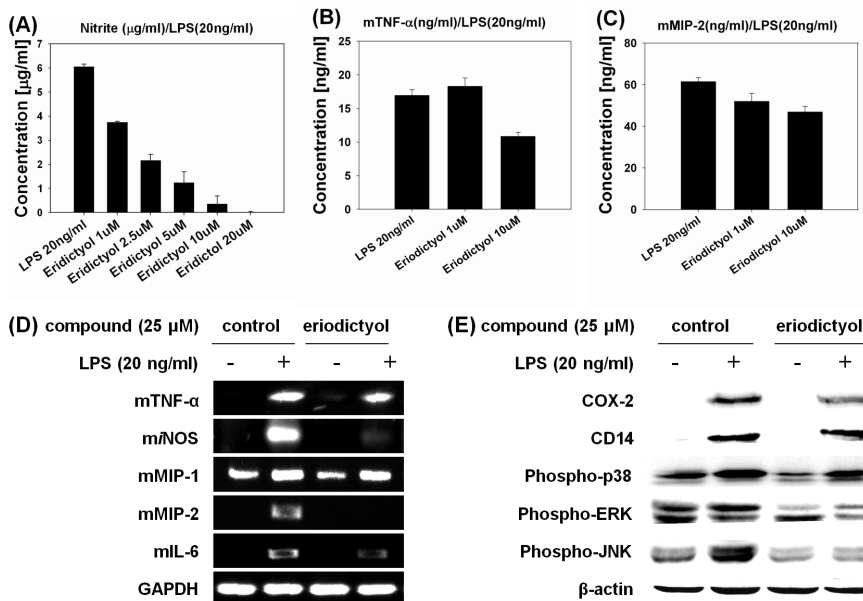


**Fig. 2.** (A) Inhibition of nitrite production by eriodictyol in LPS-stimulated RAW264.7 cells. (B) Inhibition of mTNF-α inflammatory cytokine production by eriodictyol in LPS-stimulated RAW264.7 cells. (C) Inhibition of mMIP-2 inflammatory cytokine production by eriodictyol in LPS-stimulated RAW264.7 cells. (D) Effects of eriodictyol on LPS-induced expression of inflammatory cytokines in RAW264.7 cells. Total RNA was analyzed for the expression of mIL-6, mMIP-1, mMIP-2, mTNF-α, miNOS, and GAPDH (loading control) mRNA by RT-PCR. (E) Effects of eriodictyol on CD14, COX-2, phospho-p38, phospho-ERK, phospho-JNK and β-actin. CD14, COX-2, phospho-p38, phospho-ERK, phospho-JNK and β-actin protein levels were determined by western blot analysis using specific antibodies. The relative protein expression was quantified using ImageJ (NIH, Bethesda, MD, USA).

## Quantification of inflammatory cytokines (mTNF-α and mMIP-2) in LPS-stimulated RAW264.7 cells

The inflammatory-induced cytokines that were directly measured in this study were mTNF-α and mMIP-2. The concentration of mMIP-2 cytokine sequentially decreased from 15.5% to 23.7% as the concentration of eriodictyol is increased from 1 μM to 10 μM compared with cells that were not treated with eriodictyol (Fig. 2C). In eriodictyol-treated macrophages, the levels of mTNF-α decreased 56.2% at the 10 μM concentration (Fig. 2B).

## Reverse transcription-polymerase chain reaction (RT-PCR)

When 20 ng/ml LPS was added to RAW264.7 cells, the expression of inflammatory cytokines in macrophages was detected by RT-PCR. As shown in Fig. 2D, the production of all tested cytokines, with the exception of mMIP-1, in LPS-stimulated macrophages were dramatically increased compared with macrophages without LPS stimulation. The expression of mMIP-2 cytokines were inhibited perfectly in macrophages treated with 25 μM eriodictyol and LPS. In addition, the expression of miNOS and mIL-6 mRNA was effectively suppressed 86.9% and 63.1%, respectively, compared to the mRNA levels in non-treated cells. The levels of mTNF-α and mMIP-1 decreased 17.9% and 14.5%, respectively, compared with the levels in non-treated cells.

## Western blotting

RAW264.7 cells were treated with eriodictyol with or without LPS, and a western blot was performed to detect MAPKs as well as CD14 and COX-2. The phosphorylation of p44 and p42 of ERK were significantly reduced 73.5% and 54.7%, respectively, in mouse macrophages treated with 25 μM eriodictyol. The expression of p38 MAPK and JNK were suppressed 14% and 74%, respectively. The binding of LPS to CD14 and TLR4, which is the receptor complex, is responsible for the induction of the pro-inflammatory response, including the release of NO, TNF-α, iNOS, pro-inflammatory related cytokines, and COX-2. In LPS-stimulated cells, active NF-κB translocates into the nucleus and binds to the target DNA element to activate transcription of pro-inflammatory genes such as iNOS, COX-2, and TNF-α. Our results revealed that only an 11% decrease in CD14 expression was observed in LPS-stimulated cells following pretreatment with eriodictyol. Here, a significant increase in COX-2 protein expression was observed in LPS-stimulated RAW264.7 cells compared with cells that were not exposed to LPS. Cells pretreated with eriodictyol were inhibited 39.6% by COX-2 expression. Therefore, eriodictyol was shown to inhibit NO production via decreasing the MAPKs, CD14/TLR4, and COX-2 signaling cascade.

## Fluorescein isothiocyanate (FITC)-labeled LPS aggregates

Interactions between eriodictyol and LPS indicate the dissociation of LPS aggregates, an effect that can be monitored using FITC-conjugated LPS to detect changes in fluorescence. As shown on Fig. 3A, the addition of eriodictyol caused a dose-dependent increase in FITC-LPS fluorescence, implying that eriodictyol dissociated the large LPS aggregates. This likely results in its anti-inflammatory activities.

## Fluorescence quenching

We assessed binding constants for eriodictyol binding to JNK by using fluorescence quenching experiments. As shown in Fig. 3B, the fluorescence intensity was altered with increased eriodictyol concentration. The binding affinity of the eriodictyol was estimated to be $8.79 \times 10^5 \, M^{-1}$.

## STD-NMR experiment

To investigate the mode of eriodictyol interaction with JNK, we performed STD-NMR experiments to support the site-specific binding information of the ligand in the active site of JNK. In the STD-NMR spectra of eriodictyol, $^1H$ signals of the B-ring (2', 5' and 6') were reduced 47% and 49%, respectively, whereas $^1H$ spectra of the C-ring (6 and 8) were decreased 78%, and that of the A-ring (2) was decreased 92% after saturation transfer (Fig. 4A). It may be possible that the B-ring of eriodictyol is mainly responsible for the binding interaction with the ATP-binding site of JNK, but the A-ring and C-ring do contribute, albeit less, to the binding of eriodictyol.
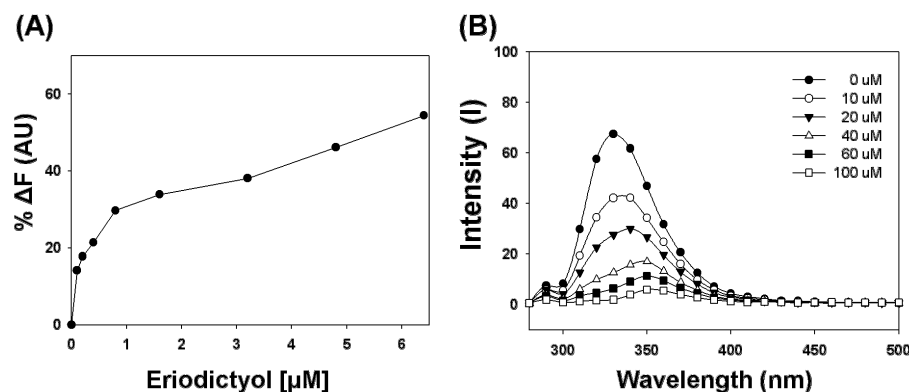


**Fig. 3.** (A) Enhancement of the intensity of FITC-labeled LPS as a function of eriodictyol concentration. (B) Fluorescence spectra of JNK in the presence of eriodictyol (0, 10, 20, 40, 60, and 100 μM) at pH 7.0. The sample was excited at 290 nm, and emission spectra recorded for light scattering effect at 290 to 600 nm.
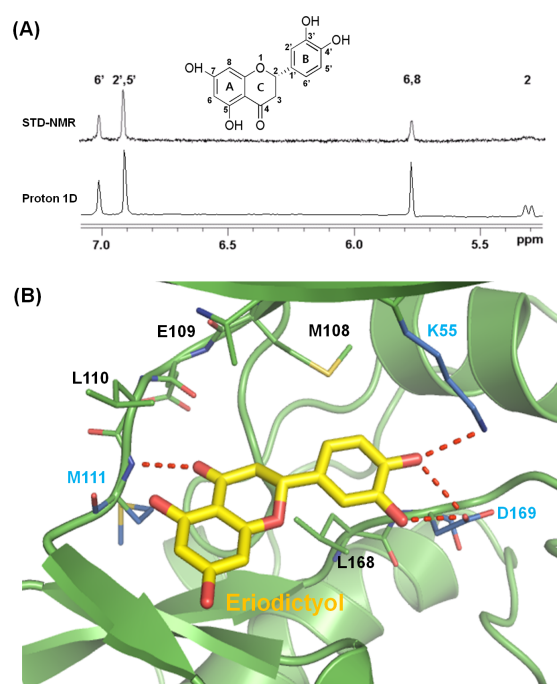
**Fig. 4.** (A) ¹H NMR for eriodictyol and representative result of the STD-NMR binding assay for eriodictyol. (B) Docking model of eriodictyol and JNK. Hydrogen bonds are depicted as red dashed lines.

## Docking study

To evaluate several biological assays and propose a binding model for eriodictyol and JNK, we performed docking with eriodictyol. Eriodictyol docked into the ATP-binding active site of JNK. We investigated the importance of the hydrogen bonds that participate in the interaction between eriodictyol and JNK. Eriodictyol has 3'-OH and 4'-OH groups, and these 2 hydroxyl groups formed hydrogen bond interactions with JNK; 3'-OH and 4'-OH formed hydrogen bonds with $O^{\delta 2}$ of Asp169 and 4'-OH also binds to $N^{\xi}$ of Lys55. The carbonyl oxygen at the 5th position of eriodictyol participated in a hydrogen bond interaction with the backbone amide of Met111, as shown in Fig 4B. This binding model is in good agreement with the results from the STD-NMR experiments of eriodictyol and JNK.

## DISCUSSION

Macrophages are involved in host defense and are closely related with inflammation targeting for binding with LPS. LPS mediates the inflammatory response by activating ERKs, p38 MAPK, and JNKs. Xagorari and his coworkers reported that flavonoid, quercetin and luteolin effectively inhibited TNF-α release in LPS-stimulated macrophages (16). In addition, it has been observed that eriodictyol, found in many kinds of fruits, has anti-inflammatory activities (15). In order to characterize whether eriodictyol inhibits LPS signaling and the in-

flammatory cascade, we further investigated gene expression at the mRNA level and inflammatory cytokine production using western blot analysis for LPS-stimulated macrophages.

Nitrite accumulation in culture media was used as an indicator of NO production. To assess the potential anti-inflammatory activity of papiliocin, we indirectly measured peptide inhibition of NO production in RAW264.7 macrophages stimulated with LPS by quantifying nitrite concentration. We clearly demonstrated that eriodictyol thoroughly inhibits NO production in LPS-stimulated macrophages at nontoxic concentrations. We also investigated the expression of miNOS, mTNF-α, mMIP-1, mMIP-2, and mIL-6 cytokines by RT-PCR. The iNOS enzyme is known to participate in anti-microbial and anti-tumor activities, and TNF-α is generally known to induce neutrophil proliferation during inflammatory events. MIP-1 and MIP-2 are included in chemotactic cytokines and are related to the immune response during infection and inflammation. IL-6 is an interleukin that is produced by T cells to stimulate immune reactions. These cytokines play a pivotal function in inflammation. The expression of the tested cytokines were considerably inhibited in LPS-stimulated macrophages by eriodictyol. Along with RNA expression, we tested the expression of ERK, p38 MAPK, and JNK, as well as CD14 and COX-2, by western blot. The eriodictyol regulated LPS-induced phosphorylation of p38, ERK, and JNK. Fig. 2E shows that the phosphorylation p38 MAPK, ERKs, and JNK are upregulated only by treatment with LPS, and that phosphorylation is downregulated by treating cells simultaneously with LPS and eriodictyol. We also observed that LPS-induced stimulation of CD14 and COX-2 is suppressed by treatment with eriodictyol. Therefore, eriodictyol was shown to inhibit NO production via decreasing CD14 following the p38 MAPK, ERK, JNK, and COX-2 signaling cascade. Accordingly, inflammatory cytokine release depends on LPS binding to CD14 associated with TLR4, indicating that the MAPK, ERK, JNK, and COX-2 pathway might be the proper target for therapeutic approaches to inflammatory diseases.

Furthermore, the FITC-conjugated LPS assay showed that the association between eriodictyol and LPS resulted in the dissociation of the LPS aggregates. Data from STD-NMR and fluorescence quenching experiments correlated well with the ligand docking results. Eriodictyol, with good anti-inflammatory activities, showed good binding affinity to JNK at $8.79 \times 10^{5} M^{-1}$. From the docking study, a binding model of eriodictyol and JNK was proposed, and the 3'-OH and 4'-OH of the B-ring as well as oxygen at the 5th position of eriodictyol are responsible for hydrogen bonding with the JNK active site. In conclusion, we proposed that eriodictyol is a potent anti-inflammatory inhibitor of JNK without cytotoxicity to mammalian cells. The JNK signaling pathway plays an important function in anti-inflammatory activities, and we have shown that eriodictyol targets JNK. The results suggest that the inhibitory effect of eriodictyol on the pro-inflammatory cytokines is likely dependent on signaling through p38 MAPK, ERK, JNK, COX-2, and CD14.

Nevertheless, the inflammatory cascade is very complicated

and sophisticated, and we will study it systematically to determine further mechanisms of action for the inflammatory activity of eriodictyol in the future.

## MATERIALS AND METHODS

### Reagents
Eriodictyol (Fig. 4A) was obtained from Fluka (Buchs, Switzerland) and dissolved in $H_2O$ : DMSO (9 : 1, v/v) at 10 mg/ml for the stock solution.

### Cytotoxicity in mammalian cells
The mouse macrophage-derived RAW264.7 cell line, mouse embryonic fibroblast NIH3T3, and human keratinocyte HaCaT cell lines were purchased from the American Type Culture Collection (Manassas, VA, USA). The cytotoxicity of eriodictyol in RAW264.7, NIH3T3, and HaCaT cells was determined as reported previously (17).

### Quantification of nitrite production in LPS-stimulated RAW264.7 cells
Nitrite accumulation in culture media was used as an indicator of NO production, and NO production was determined as described previously (18).

### Quantification of inflammatory cytokines (mTNF-α and mMIP-2) in LPS-stimulated RAW264.7 cells
Antibodies against mTNF-α and mMIP-2 were used for immobilization on immune plates as reported previously (19).

### Reverse transcription-polymerase chain reaction
RAW264.7 cells were stimulated without (negative control) or with 20 ng/ml LPS in the presence or absence of eriodictyol for 3 h. Competitive RT-PCR was performed as described previously (20). The targets were amplified from the resulting cDNA by PCR using the following specific primers: mIL-6, 5′-ACA AGT CCG GAG AGG AGA CT-3′ (sense) and 5′-GGA TGG TCT TGG TCC TTA GC-3′ (antisense); mMIP-1, 5′-ATG AAG CTC TGC GTG TCT GC-3′ (sense) and 5′-TGA GGA GCA AGG ACG CTT CT-3′ (antisense); mMIP 2, 5′-ACA CTT CAG CCT AGC GCC AT-3′ (sense) and 5′-CAG GTC AGT TAG CCT TGC CT-3′ (antisense); mTNF-α, 5′-GTT CTG TCC CTT TCA CTC ACT G-3′ (sense) and 5′-GGT AGA GAA TGG ATG AAC ACC-3′ (antisense); miNOS, 5′-CTG CAG CAC TTG GAT CAG GAA CCT G-3′ (sense) and 5′-GGG AGT AGC CTG TGT GCA CCT GGA A-3′ (antisense). The primers for glyceraldehyde 3-phosphate (GAPDH), used as an internal control, were 5′-ACC ACA GTC CAT GCC ATC AC-3′ (sense) and 5′-TCC ACC ACC CTG TTG CTG TA-3′ (antisense). PCR was performed using the following cycling conditions: 94$^o$C for 5 min, followed by 25 cycles of 94$^o$C for 1 min, 55$^o$C for 1.5 min and 94$^o$C for 1 min, and a final extension step of 72$^o$C for 5 min.

### Western blotting
The proteins were isolated from LPS-stimulated RAW264.7 cells with or without eriodictyol, and signals were detected as reported previously (21). Antibodies were used specifically for phospho-ERK (1 : 2,000; Cell Signaling Technology, Beverly, MA, USA), phospho-p38 (1 : 2,000, Cell Signaling Technology), CD14 (1 : 200, Santa Cruz, Dallas, TX, USA), JNK and COX-2 (1 : 1,000, Cell Signaling Technology), and β-actin (1 : 5,000, Sigma-Aldrich, St. Louis, MO, USA). The relative amount of protein associated with each antibody was quantified using ImageJ (NIH, Bethesda, USA).

### FITC-labeled LPS aggregates
The interactions between eriodictyol and FITC-conjugated LPS were studied by exciting 0.5 μM FITC-LPS at 480 nm and monitoring the change in the emission of FITC at 515 nm in the presence of different concentrations of eriodictyol.

### Construction of expression plasmids and JNK1Protein purification
To express JNK1 for structural analysis, the C-terminal truncated form of human JNK1α1 (residues 1-364) was cloned into pET21b expression vector (Novagen) and expressed in Escherichia coli as a 6 His-tagged form at the C-terminus. JNK1 was purified as reported previously (22).

### STD-NMR
The protein was saturated on-resonance at -1.0 ppm and off-resonance at 30 ppm, with a cascade of 40 selective Gaussian-shaped pulses of 50 ms duration and 100 ms delay between each pulse in all STD-NMR experiments at 298 K. The total duration of the saturation time was set to 2 s. For STD-NMR experiments, 10 μM recombinant JNK in 50 mM sodium phosphate buffer, 100 mM NaCl, pH 8.0, and candidate inhibitors were mixed at a protein:ligand ratio of 1 : 100. In total, 1024 scans for each experiment were acquired, and a WATERGATE sequence was used to suppress the water signal. A spin-lock filter (5 kHz strength and 10 ms duration) was applied to suppress the protein background. All NMR spectra were recorded on a Bruker Avance 500 MHz NMR spectrometer at KBSI.

### Fluorescence quenching
We titrated each candidate inhibitor to 10 μM JNK protein solution in 50 mM sodium phosphate buffer containing 100 mM NaCl at pH 8.0, with a final protein:inhibitor ratio of 1 : 10. The sample was placed in a 2 ml cuvette, with excitation and emission path lengths of 10 nm. Using tryptophan emission, we determined the fluorescence quantum yields of JNK and the ligand. The methods were performed as described in detail previously (12).

### Docking study
Using the X-ray crystallography structure of JNK (3v3v.pdb), we

defined the ATP-binding site of JNK. Eriodictyol was docked to JNK using CDOCKER, a CHARMm-based molecular dynamics (MD) method for ligand-docking, in Discovery Studio modeling (Accelrys Inc., San Diego, USA). This algorithm assumes a rigid protein and permits only the ligand to be flexible. The Input Site Sphere parameter specifies a sphere around the center of the binding site, where the CDOCKER experiment is to be performed. The center of the sphere is used in the CDOCKER algorithm for initial ligand placement. The MD simulated annealing process is performed using a rigid protein and flexible ligand. The final minimization step is applied to the ligand's docking pose. The minimization consists of 50 steps of steepest descent followed by up to 200 steps of conjugated-gradient using an energy tolerance of 0.001 kcal/mol (23).

## Acknowledgements

## REFERENCES

1. Ferrero-Miliani, L., Nielsen, O. H., Andersen, P. S. and Girardin, S. E. (2007) Chronic inflammation: importance of NOD2 and NALP3 in interleukin-1beta generation. *Clin. Exp. Immunol.* **147**, 227-235.

2. Ma, Y. J., Kang, H. J., Kim, J. Y., Garred, P., Lee, M.-S. and Lee, B. L. (2013) Mouse mannose-binding lectin-A and ficolin-A inhibit lipopolysaccharide-mediated pro-inflammatory responses on mast cells. *BMB Rep.* **46**, 376-381.

3. Stichtenoth, D. O. and Frolich, J. C. (1998) Nitric oxide and inflammatory joint diseases. *Br. J. Rheumatol.* **37**, 246-257.

4. Kim, S., Jung, E., Shin, S., Kim, M., Kim, Y.-S., Lee, J. and Park, D. (2012) Anti-inflammatory activity of *Camellia japonica* oil. *BMB Rep.* **45**, 177-182.

5. Chen, W., Tang, Q., Gonzales, M. S. and Bowdwn, G. T. (2001) Role of p38 MAP kinase and ERK in mediating ultraviolet-B induced cyclooxygenase-2 gene expression in human keratinocytes. *Oncogene.* **20**, 3921-3926.

6. Dauchet, L., Ferrieres, J., Arveiler, D., Yarnell, J. W., Gey, F., Ducimetiere, P., Ruidavets, J. B., Haas, B., Evans, A., Amouyel, P. and Dallogeville, J. (2004) Frequency of fruit and vegetable consumption and coronary heart disease in France and Northern Ireland: the PRIME study. *Br. J. Nutr.* **92**, 963-972.

7. Di carlo, G., Mascolo, N., Izzo, A. A. and Capasso, F. (1999) Flavonoids: old and new aspects of a class of natural therapeutic drugs. *Life Sci.* **65**, 337-353.

8. Cunningham, B. D., Threadgill, M. D., Groundwater, P. W., Dale, I. L. and Hickman, J. A. (1992) Synthesis and biological evaluation of a series of flavones designed as inhibitors of protein tyrosine kinases. *Anticancer Drug Des.* **7**, 365-384.

9. Kim, O. K., Murakami, A., Nakamura, Y. and Ohigashi, H. (1998) Screening of edible Japanese plants for nitric oxide generation inhibitory activities in RAW264.7 cells. *Cancer Lett.* **125**, 199-207.

10. Lee, E., Shin, S., Kim, J.-K., Woo, E.-R. and Kim, Y. (2012) Anti-inflammatory effects of amentoflavone on modulation of signal pathway in LPS-stimulated RAW264.7 cells. *Bull. Korean Chem. Soc.* **33**, 2878-2882.

11. Ismaili, H., Sosa, S., Brkic, D., Fkih-Tetouani, S., Ilidrissi, A., Touati, D., Aquino, R. P. and Tubaro, A. (2002) A topical anti-inflammatory activity of extracts and compounds from *Thymus broussonettii*. *J. Pharm. Pharmacol.* **54**, 1137-1140.

12. Minato, K., Miyake, Y., Fukumoto, S., Yanamoto, K., Kato, Y., Shimomura, Y. and Osawa, T. (2003) Lemon flavonoid, eriocitrin, suppresses exercise induced oxidative damage in rat liver. *Life Sci.* **72**, 1609-1616.

13. Lee, J.-Y. Lee, J. Jeong, K.-W. Lee, E. and Kim, Y. (2011) Flavonoid Inhibitors of β-Ketoacyl Acyl Carrier Protein Synthase III against Methicillin-Resistant *Staphylococcus aureus*. *Bull. Korean Chem. Soc.* **32**, 2695-2699.

14. Jeong, K.-W., Lee, J.-Y., Kang, D.-I., Lee, J.-U., Shin, S. Y. and Kim, Y. (2009) Screening of flavonoids as candidate antibiotics against *Entrococcus faecalis*. *J. Nat. Prod.* **72**, 719-724.

15. Lee, J. K. (2011) Anti-inflammatory effects of eriodictyol in lipopolysaccharide-stimulated Raw 264.7 murine macrophages. *Arch. Pharm. Res.* **34**, 671-679.

16. Xagorari, A., Papapetropoulos, A., Mauromatis, A., Economou, M., Fotsis, T. and Roussos, C. (2000) Luteolin inhibits an endotoxin-stimulated phosphorylation cascade and proinflammatory cytokine production in macrophages. *JEPT* **296**, 181-187.

17. Scudiero, D. A., Shoemaker, R. H., Paull, K. D., Monks, A., Tierney, S., Nofziger, T. H., Currens, M. J., Seniff, D. and Boyd, M. R. (1988) Evaluation of a soluble tetrazolium/formazan assay for cell growth and drug sensitivity in culture using human and other tumor cell lines. *Cancer Res.* **48**, 4827-4833.

18. Green, L. C., Wagner, D. A., Glogowski, J., Skipper, P. L., Wishnok, J. S. and Tannenbaum, S. R. (1982) Analysis of nitrate, nitrite, and [15N] nitrate in biological fluids. *Anal. Biochem.* **126**, 131-138.

19. Kim, K. H., Shim, J. H., Seo, E. H., Cho, M. C., Kang, J. W., Kim, S. H., Yu, D. Y., Song, E. Y., Lee, H. G., Sohn, J. H., Kim, J. M., Dinarello, C. A. and Yoon, D. Y. (2008) Interleukin-32 monoclonal antibodies for Immunohistochemistry, Western blotting, and ELISA. *J. Immunol. Methods* **333**, 38-50.

20. Jeon, Y. J., Han, S. B., Ahn, K. S. and Kim, H. M. (1999) Activation of NF-kappaB/Rel in angelanstimulated macrophages. *Immunopharmacology* **43**, 1-9.

21. Jung, H. W., Mahesh, R., Park, J. H., Boo, Y. C., Park, K. M. and Park, Y.-K. (2010) Bisabolangelone isolated from *Ostericum koreanum* inhibits the production of inflammatory mediators by down-regulation of NF-κB and ERK MAP kinase activity in LPS-stimulated RAW264.7 cells. *Int. Immunopharmacol.* **10**, 155-162.

22. Heo, Y.-S., Kim, S.-K., Seo, C. I., Kim, Y. K., Sung, B.-J., Lee, H. S., Lee, J. I., Park, S.-Y., Kim, J. H., Hwang, K. Y., Hyun, Y.-L., Jeon, Y. H., Ro, S., Cho, J. M., Lee, T. G. and Yang, C.-H. (2004) Structural basis for the selective inhibition of JNK1 by the scaffolding protein JIP1 and SP600125. *EMBO J.* **23**, 2185-2195.

23. Vieth, M., Hirst, J. D., Dominy, B. N., Daigler, H. and Brooks, C. L. (1998) Assessing search strategies for flexible docking. *J. Comput. Chem.* **19**, 1623-1631.